On the Potential of Direct and MHD Conversion of Power from a Novel Plasma Source to Electricity for Microdistributed Power Applications

R. M. Mayo,[a)] R. L. Mills, and M. Nansteel

BLP Inc.,

Cranbury, NJ 08512

The generation of electricity using direct electrostatic and magnetohydrodynamic (MHD) conversion of the plasma particle energy of small to mid-size chemically assisted microwave or glow discharge plasmas (CA-plasma) power sources in the range of a few hundred Watts to several 10's of kW for microdistributed commercial applications (e.g. household, automotive, light industry, and space based power) is studied for the first time. In the determination of the effect of plasma parameters on conversion efficiency, careful attention was paid to the unique plasma conditions of low pressure, low ionization fraction, and nonthermal ion energies that are much greater than that of the thermal ions of traditional MHD but much lower than those of a fully ionized plasma typically generated for fusion experiments. The density of plasma ions and neutrals and their cross sections for processes such as charge exchange were also considered. The most important parameters were found to be charged particle density and energy, as well as the large inventory of neutral gas atoms and molecules. Momentum and charge exchange of plasma ions with the large background fraction of neutrals represents a limitation to conversion efficiency. Two conversion technologies were examined in some detail. We considered the possibility of converting a CA-plasma using adaptations of a member of the broad category of electromagnetic direct converters previously developed for recovery and conversion of the high energy particles lost from tandem mirror and magnetically confined plasmas, and an MHD converter previously developed for conversion of high pressure combustion gases to electricity. While it was found that both conversion techniques performed well under ideal conditions for conversion of plasma to electricity showing conversion efficiencies of $> 50\%$, the tight coupling of plasma cell and converter, size limitations, particle energy, and the substantial inventory of relatively low energy neutrals eliminate direct electrostatic converters

as practical converters under these conditions. However, MHD conversion of CA-plasmas appears feasible at ~50% efficiency with a simple compact design.

I. INTRODUCTION

Central station generation and distribution, the mainstay of electrical power production for the last 100 years worldwide, is now being supplemented in an increasing number of areas by smaller power units closer to the end-user group. Most distributed-generation units are in the capacity range of 100 kW–3 MW (electric), but some could be as large as 250 MW (electric). Distributed generation solves some of centralized power's inherent problems of transmission and distribution line losses, electromagnetic pollution fears from high-tension lines, cost and difficulty of transmission-line maintenance, and inefficiencies in load factor design of power plants (wherein the use of a 20% capacity safety factor is still a common industry practice when estimating peak loading).

The microdistributed market emerged with uninterruptable power supplies (UPS) which serve the premium power market including businesses where brief electrical outages can cause severe monetary loss: telecommunication sites, computer centers, server hotels, e-commerce centers, semiconductor fabrication facilities, and others. With a suitable technology, market conditions exist to extend the trend away from central power with the expansion of microdistributed power into the broader electricity market. The broader market which includes hundreds of millions of homes and businesses in the US, Europe, and Japan will be drawn by significant cost savings and increasing unreliability of the grid with a lack of viable microdistributed alternatives. The market is already moving in that direction. Plug Power[1] is developing a home fuel cell unit for the U.S. market, and in Japan, Matsushita plans to introduce a 1 kW fuel-cell system costing $10,000 where the price of electricity is 20 /kW-hr for microdistributed power.[2] The current price for government subsidized green distributed power in Germany is even higher, 50 /kW hr.[3] The populace of the third world, particularly Asia, represents a further enormous market opportunity for a technology with low capital and O&M costs and no requirement of an electrical grid infrastructure.

The automotive market is also currently at a crossroads with many different options being considered for the next generation of automobile. Evidence of the changing landscape for automobiles can be found in the recent increase in research into the next generation of automobiles. But, the fact that there is no clear front-runner in the technological race to replace the internal combustion

(IC) engine can be attested to by the divergent approaches taken by the major automobile companies. Programs include various approaches to hybrid vehicles, alternative fueled vehicles such as dual-fired engines that can run on gasoline or compressed natural gas, and a natural gas-fired engine. Serious efforts are also being put into a number of alternative fuels such as ethanol, methanol, propane, and reformulated gasoline. To date, the most favored approach is an electric vehicle based on fuel cell technology or advanced battery technology such as sodium nickel chloride, nickel-metal hydride, and lithium-ion batteries.[4] Although billions of dollars are being spent to develop an alternative to the IC engine, there is no technology in sight that can match the performace of an IC engine system.[5]

A chemically generated or assisted plasma (CA-plasma) as a novel power source using hydrogen as the fuel has been reported previously.[6–11] Since the power is in the form of a plasma, high-efficiency, low-cost direct energy conversion may be possible, thus, avoiding a heat engine such as a turbine[12,13] or a reformer-fuel-cell system. Significantly lower capital costs and lower commercial operating costs than that of any known competing energy source are anticipated.

High temperature plasmas possess a substantial inventory of energy stored in the thermal and/or kinetic components of plasma ions, electrons, and in some cases neutral gas particles in some weakly ionized plasmas. There is obvious incentive then in devising methods and technologies to efficiently extract this energy and convert it to a more useful form. Most often, conversion to electrical energy is desired as this form is readily stored and transmitted, and is efficiently converted to mechanical work at the delivery site.

A number of conversion schemes have been studied in the four plus decades of controlled thermonuclear fusion research. At high temperature (as that produced in the blanket material of high power D-T fusion reactor) a thermal steam cycle[14,15] is usually considered the most practical energy extraction means as the bulk (80%) of the energy release is in the form of chargless neutrons. Thermal steam cycles are robust, reliable, proven technologies, and are well established as the work horse of modern electrical power delivery. Yet, the conversion efficiency is limited and high coolant temperatures are required. Furthermore, costs are prohibitive for the use of steam cycles in small, distributed power sources.

Direct conversion of plasma charged particle kinetic to electric energy[16] may represent an attractive alternative to the steam cycle for at least several plasma systems of great interest including; (a) the D-T fusion reactor (as a "topping" unit to extract the 20% of fusion energy in high energy charged particles), (b) advanced, a-neutronic fueled fusion reactors, and (c) CA-plasma cells. In fusion reactors, the fully ionized, high temperature (up to 10–15 keV) plasma energy may be readily extracted by direct, electrostatic means, thereby converting charged particle kinetic energy to electrostatic potential energy via decelerating electrodes.[16] Whereas for CA-plasma cell devices, possessing only weakly ionized and relatively cold plasmas, conversion methods more compatible with a fluid environment like MHD converters may be required to extract stored energy.

A number and variety of direct energy conversion techniques have been studied over the years.[16] Many of these may be loosely grouped into the following broad catagories. (1) Electrostatic Direct Converters: Electrostatic direct devices convert directed ion kinetic energy to electrical potential energy via an electrode (or set of electrodes) electrically biased to decelerate ions extant from the plasma source. The most well studied of such converter devices are the *venetian blind*[17,18] and *periodic focused*[19] converters. These devices appear to hold great promise as very efficient (80–90%) direct converters for large scale (on the order of 1000 MW) generating stations. In these devices, plasma particles are electrostatically separated before deceleration and collection at the electrodes. Separation incurs space charge limitations which are particularly troublesome for all but very high energy particles. Reasonable currents are achievable only at very high energy (several to 100s of keV). Particles of these energy levels are not present in appreciable numbers in CA-plasma cells. Furthermore, to mitigate the effects of high heat loading,[20,21] such devices require plasma expansion and become enormous in linear scale (10's–100's of meters).

(2) Electromagnetic Direct (Crossed Field or Drift) Converters: The guiding center drift of charged particles in magnetic and crossed electric fields may be exploited to separate and collect charge without the necessity to do so electrostatically. Space charge complications are to a large degree eliminated. Dimensions can often be reduced (for low power converters) by many orders (perhaps to the ion gyro-scale). Natural mating of the converter magnetic field to a guide field is a further advantage. As the devices extract particle energy perpendicular to the magnetic field, expansion

may not be necessary and is often undesirable. The performance characteristics of an idealized $\vec{E} \times \vec{B}$ converter which relies on the inertial difference between ions and electrons, is analyzed in sec. III. Timofeev[22,23] devised a high efficiency conversion device based on combined $\vec{E} \times \vec{B}$ and $\nabla \vec{B}$ drift collection. This particular device is again designed for high-power fusion energy conversion and is quite large in dimension, and requires expansion and end plug fields to prevent plasma leakage. In addition, collisions among energetic ions and neutral particles in a low power plasma cell will likely interrupt the drift trajectory required for efficient energy conversion. As an example, Ar^+ ions in a 1 T field have a gyro-frequency of $\omega_{c_i} \sim 2.4 \times 10^6$ s^{-1} and a collision frequency with neutral Ar atoms of $\nu_{in} \sim 6 \times 10^7$ s^{-1} at 40 eV, making the ion magnetization parameter $\Omega = \omega_c/\nu \sim 0.04$. (For H^+ ions under the same conditions the magnetization parameter is 0.27). Ions then are readily interrupted in their drift trajectory and will not reach the desired collection electrode in the $\nabla \vec{B} \times \vec{B}$ direction.

(3) MHD Converter: In MHD a highly conducting plasma, flowing at velocity $\vec{u}$ in a direction across a magnetic field $\vec{B}$ gives rise to an electric field $\vec{E} = -\vec{u} \times \vec{B}$. This electric field may be intercepted at the boundary of a plasma device by electrodes and exploited to drive electric current through an external load. Mechanical flow energy of the conducting fluid is then converted to electrical energy. In the presence of a load to complete the circuit, the density of electric current, $\vec{j}$, is given by the plasma Ohm's law

$$\vec{j} = \sigma(\vec{E} + \vec{u} \times \vec{B}) \tag{1}$$

where σ is the plasma electrical conductivity. The term is $\vec{u} \times \vec{B}$ is referred to as the MHD electric field or MHD term in Ohm's law.

The performance of an MHD power conversion system is impacted strongly by the value of σ attained in the plasma region of the MHD converter. As such, collisions among charge carriers or between charge carriers and neutral gas atoms play a crucial role. Collisions, however, are not as disruptive in MHD converters as they are in direct conversion. MHD converters operate on fluid plasmas where collisions are frequent and the trajectories of individual plasma particles are relatively unimportant. The conductivity is also affected strongly by the strength of applied magnetic field in plasma. A more detailed discussion of this subject is presented in sec. IV. MHD

Power conversion devices acting on alkali metal seeded, high-pressure (at or above atmospheric) combustion gases have been extensively studied[24-29] including MHD concepts to deliver AC power directly from the converter.[30,31] Prior studies also include plasmas generated in shock tubes or arc jets for high power electric generation. Little effort has been made in studying MHD conversion in hotter, more tenuous plasmas for low power applications. The work described herein is intended to initiate such a dialogue.

II. PROPERTIES OF CA-PLASMA CELLS & CONVERTER CONCERNS

A. Plasma Parameters

Plasma cells operating at about 1 Torr total pressure in the glow or microwave discharge regime producing output power significantly greater than the input power due to catalytic release of energy from supplied hydrogen have been reported previously.[6-11] Results from studies on ca-plasmas of hydrogen with strontium, argon or helium with 3–10% hydrogen and strontium with these latter mixtures include:

1. the observation that glow discharge plasmas of the catalyst-hydrogen mixtures of strontium-hydrogen, helium-hydrogen, argon-hydrogen, strontium-helium-hydrogen, and strontium-argon-hydrogen showed significant Balmer-α line broadening corresponding to an average hydrogen atom temperature of 25–45 eV; whereas, plasmas of the noncatalyst-hydrogen mixtures of pure hydrogen, krypton-hydrogen, xenon-hydrogen, and magnesium-hydrogen showed no excessive broadening corresponding to an average hydrogen atom temperature of $\sim$ 3 eV,[10,11]

2. the observation that microwave helium-hydrogen and argon-hydrogen plasmas having catalyst Ar^+ or He^{2+} showed extraordinary Balmer-α line broadening due to hydrogen catalysis corresponding to an average hydrogen atom temperature of 110–130 eV and 180–210 eV, respectively; whereas, plasmas of pure hydrogen, neon-hydrogen, krypton-hydrogen, and xenon-hydrogen showed no excessive broadening corresponding to an average hydrogen atom temperature of $\sim$ 3 eV,[7,10]

3. the observation that microwave helium-hydrogen and argon-hydrogen plasmas showed average electron temperatures that were high, 28,000 K and 11,600 K, respectively; whereas, the corresponding temperatures of helium and argon alone were only 6800 K and 4800 K, respectively,[7,10]

4. the observation that the optically measured output power of gas cells for power supplied to the glow discharge increased by over two orders of magnitude depending on the presence of less than 1% partial pressure of certain catalysts in hydrogen gas or argon-hydrogen gas mixtures, and an excess thermal balance of 42 W was measured for the 97% argon and 3% hydrogen mixture versus argon plasma alone,[6]

5. the observation that the power output exceeded the power supplied to a hydrogen glow discharge plasmas by 35–184 W depending on the presence of catalysts helium or argon and less than 1% partial pressure of strontium metal in noble gas-hydrogen mixtures; whereas, the chemically similar noncatalyst krypton had no effect on the power balance,[11]

6. the Calvet calorimetry measurement of an energy balance of over -151,000 kJ/mole-H_2 with the addition of 3% hydrogen to a plasma of argon having the catalyst Ar^+ compared to the enthalpy of combustion of hydrogen of -241.8 kJ/mole-H_2; whereas, under identical conditions no change in the Calvet voltage was observed when hydrogen was added to a plasma of noncatalyst krypton,[8]

7. the observation that upon the addition of 10% hydrogen to a helium microwave plasma maintained with a constant microwave input power of 40 W, the thermal output power was measured to be at least 400 W corresponding to a reactor temperature rise from room temperature to 1200 °C within 150 seconds, a power density of 40 MW/m^3, and an energy balance of at least -5×10^5 kJ/mole-H_2 compared to the enthalpy of combustion of hydrogen of -241.8 kJ/mole-H_2,[9]

Plasma parameters of a CA-plasma of an argon-hydrogen mixture (97/3%) which are very conservative in terms of their impact on the potential for conversion of plasma power to electricity are given in table 1 along with fill gas parameters at $\sim$ 1 Torr.

B. Device Scale

Practical design parameters were established for the magnetic field strength B of 1 T and a converter physical scale L of 1 m to determine the performance of the converter. Fields on this order are readily produced with Weiss electromagnets[32] with iron or rare-earth cores and without active cooling. The choice of converter length is considered a reasonable upper limit in an initial analysis of micro-distributed power devices without a detailed cost analysis. At times, the parameters B and L will be treated as independent variables for the purpose of optimization or parameterization; although, it is always recognized that practical considerations limit these to be of the order prescribed above.

C. Energy Content and Power Flow

To gauge the power scales involved, initial energy content and power flow estimates were made. At $T_e \sim 10$ eV, $T_i \sim 40$ eV; and $n_{e,i} = 10^{12}$ cm$^-3$, for a 1 liter plasma cell, the stored thermal energy is

$$U_T = n_{e,i} V (kT_e + kT_i) \sim 8\text{mJ} \tag{2}$$

independent of ion species, where V is the plasma volume. Power flow can be estimated presuming the ability to extract this stored energy at an acoustic rate. At 40 eV, H+ ions have an acoustic speed of $\sim 6 \times 10^4$ m/s, while that for Ar+ ions is $\sim 10^4$ m/s. For a 10 cm drift path through the cell, this makes the drift time for H^+ and Ar^+ ions $t \sim 1.67\mu$s and $\sim 10\mu$s, respectively. Assuming a particle replacement to maintain steady conditions of nvA, where nv is the particle outflux and A is the flow channel cross section, thermal energy can then be extracted at a rate $U_T/t \sim 4.78$ kW for H^+ and 0.8 kW for Ar^+. This analysis is identical to setting the power output equal to the kinetic energy flow rate, $mv^2(nvA)/2$. A similar argument can be made by considering the rate at which work is done on the fluid as it is expelled from the cell, $P = \partial W/\partial t \simeq Fv$ for constant F. For $F \sim pA$, then $P = pvA = nkTvA$ for an ideal gas. All of the aforementioned arguments, of course, require that steady conditions are maintained while extracting energy at the estimated rate. To do this, plasma particles must be replaced at the rate nvA and heated to steady temperature T at the rate kT/t per particle.

D. Converter Concerns

It is considered convention in the direct conversion of plasma to electrical energy that a conversion system must perform the following tasks. (1) A well defined plasma stream is extracted from the plasma confinement or reactor chamber. (2) Neutral particles must be trapped or otherwise diverted from the plasma flow to ensure high quality plasma and reduce the deleterious effects of neutral interactions including elastic scattering and charge exchange recombination. (3) The extant plasma stream must be expanded to reduce the heat loading on converter surfaces such as electrodes and grids, and convert plasma thermal energy to flow energy, thereby enhancing converter performance. (4) Charge separation is performed usually by electrostatic means. Ions and electrons are separated very early in the converter region. Before being individually collected, substantial space charge is developed which can severely limit performance especially at low energy (below a few keV). (5) Charged particles are decelerated at high voltage electrodes and collected. For high efficiency, many electrodes may be required, each set at a different bias voltage to intercept ions with kinetic energy nearly equal to the bias potential. (6) To meet the needs of the application, direct converter power (usually high voltage DC) must be conditioned to the requirements at the delivery site.

These are all challenging engineering issues for direct conversion. Neutral trapping incurs the need for diverting the plasma flow and a differential pumping system to remove the neutral inventory. Extraction may require a separate extraction chamber and additional magnetic field coils for guide fields. Expansion increases the physical dimensions and cost of the converter and supporting systems. Charge separation introduces the inevitable and sometimes fatal complication of space charge limitations.

Fortunately, however, many of these requirements are dictated by the high power and high energies per particle associated with the nuclear fusion origins of direct conversion. At lower particle energies, many of these constraints can be relaxed. For example, wall loading is not considered a materials concern at the relatively low power typical of CA-plasma cell devices. Therefore, expansion may not be necessary unless there is a compelling conversion advantage (*i.e.* greatly increased conversion efficiency). Collecting plasma thermal or flow energy directly (as in the $\vec{E} \times \vec{B}$

or MHD conversion techniques) rather than first converting this energy to directed individual particle energy, eliminates the need for charge separation. This represents an enormous advantage and, in many cases, an enabling condition for CA-plasma power converters. Space charge would otherwise pose an insurmountable obstacle. As an example, consider an infinitely wide (so that transverse space charge effects are neglected) beam of H^+ ions at 10 eV and 1.6 kA/m^2. This beam dictates a longitudinal space charge limitation on the maximum collector length of $\sim$ 0.5 mm, an obviously impractical constraint. The complications associated with plasma extraction and neutral trapping may also be eliminated by considering conversion strategies that allow the immersion of electrodes in-situ or allow a collector region to be closely coupled to the plasma cell to provide a natural flow path from cell to collector as in the case of $\vec{E} \times \vec{B}$ and MHD converters. Flow or collection interruption by neutral particles must still be considered, however.

E. Recombination

In low temperature plasmas, the recombination of free charge is often an important consideration in determining the concentration and distribution of charge states. This is especially true of low temperature plasmas that possess high neutral concentration and low ionization fraction. Three principle reactions dominate in the parameter range of interest, radiative and dielectronic recombination, and resonant charge exchange (CX). Estimating the rate of dielectric and radiative recombination is important for any plasma-to-electric conversion scheme since these processes remove free charge from the inventory intended for collection. Though the CX reaction does not alter the net concentration of ions in the plasma, it has the deleterious effect for conversion technologies relying on flow like MHD by removing energetic ions from the flow stream and replacing them with energetic neutral particles, leaving behind cold ions.

CX may occur among particles of the same species or among different species so long as the ionization energetics permits. In CA-plasma cells comprising Ar-H mixtures at low pressure in which the H minority concentration is not insignificant ($\gtrsim$ 3%), H^+ is expected to be the majority charge carrier as it is energetically favorable for ionized Ar to ionize H through CX.

The relevant recombination reactions then are those involving H^+. Radiative recombination in H^+ occurs with a rate coefficient of $\sim 10^{13}$ cm^3/s. In plasma of electron density of 10^{12} cm^{-3}, this yields a recombination frequency of 0.1 s^{-1} or a 10 s recombination time. The recombination mean free path at 40 eV is then in excess of 600 km, a completely negligible process. CX, on the other hand, occurs at a much higher rate. The CX cross section for H^+ on H^o is $\sim 10^{-16}$ cm^2. At 5% neutral H concentration, the CX mean path is then on the order of 10 cm. This is a reasonable dimension for the length of a small scale converter for a CA-plasma power cell.

III. $\vec{E} \times \vec{B}$ DIRECT CONVERTER

To illustrate an example of direct conversion for small to mid-scale power applications, the kinematics expressions and conversion efficiency are derived for the simple $\vec{E} \times \vec{B}$ converter with both ion and electron collectors. The zero order behavior of an ideal converter is described to retain an analytically tractable formalism. In the absence of significant expansion, the impact of collisions cannot be underestimated. As briefly mentioned in the introduction section, collisions may significantly reduce the efficiency of such devices by interrupting ion trajectories to the collector.

A schematic of a converter based on $\vec{E} \times \vec{B}$ collection is shown in Fig. 1. Here a rectangular arrangement of electrodes is chosen for simplicity with plasma particles incident from the left and drifting along guide field, $\vec{B}$. When both ions and electrons enter the collector region and experience the applied crossed fields, $\vec{E}$ and $\vec{B}$, they will immediately assume a guiding center drift in the direction perpendicular to both $\vec{E}$ and $\vec{B}$ and with speed $\vec{v}_E = \vec{E} \times \vec{B}$. Though this speed is identical for ions and electrons, ions having greatly reduced translational speed parallel to $\vec{B}$ (for $T_i = T_e$), will be turned and deflected to the upper electrode before electrons. For the same transit time, high-speed electrons will then be intercepted by the end electrode. The addition of electron collection increases direct power conversion.

Direct electromagnetic conversion like $\vec{E} \times \vec{B}$ offers distinct advantage over electrostatic conversion for a number of reasons. Perhaps the single most important aspect is that, like all fluid drift conversion processes, $\vec{E} \times \vec{B}$ conversion acts on the entire neutral plasma. The necessity to separate charge is thereby removed as are the space-charge complications that arise therefrom. Coupling to

the plasma source and expander (if necessary) are quite natural in an converter with its applied guide field. Furthermore, expansion may be unnecessary in this concept since the energy extraction in crossed field concepts is perpendicular to both $\vec{B}$ and the direction of plasma extraction from the source. In the absence of expansion, dimensions can be greatly reduced. Collisions and end losses remain the principle obstacles to high efficiency conversion.

To assess the benefit of expansion in an $\vec{E} \times \vec{B}$ converter, an analysis is performed on expansion kinematics and collection efficiency. All plasma and field parameters before the flow enters the expander are identified with the subscript 1, and those upon exiting the expander and entering the converter are identified with subscript 2. For plasma particles initially at total energy $W_1 = W_{\|_1} + W_{\perp_1}$, equipartition requires that $W_{\perp_1} = 2W_{\|_1}$ where $\perp$ and $\|$ refer to directions perpendicular and parallel to the guide field, respectively, so that

$$v_{\|_1} = \sqrt{\frac{kT_1}{M}} \quad , \quad v_{\perp_1} = \sqrt{\frac{2kT_1}{M}} \tag{3}$$

where M is the species mass. An expander region must conserve magnetic flux so that for cross sections of linear dimension d_1 and d_2 at the inlet and outlet of the expander respectively, we have

$$B_1 d_1^2 = B_2 d_2^2 \tag{4}$$

Assigning $d_1 = a d_2$, where a is a dimensionless, inverse expansion ratio, flux conservation can be expressed as $B_2 = a^2 B_1$. By conserving the adiabatic invariant $\mu = W_\perp / B$, expressions for the post expansion particle speed are obtained

$$v_{\perp_2} = a\sqrt{\frac{2kT_1}{M}} \quad , \quad v_{\|_2} = \left(\frac{3}{2} - a^2\right)^{1/2} \sqrt{\frac{2kT_1}{M}} \tag{5}$$

Note that when $a = 1$ (the no expansion limit) then $v_{\perp_2} = v_{\perp_1}$ and $v_{\|_2} = v_{\|_1}$.

Conserving mass flow nvA (where A is the channel cross section at any position) determines the particle density change across the expander section

$$\frac{n_2}{n_1} = \frac{a^2}{(3 - 2a^2)^{1/2}} \tag{6}$$

Coupling this result to an adiabatic expansion requirement (pV^γ =const.) and the ideal gas law ($p = nkT$), dictates a temperature difference across the expander region

$$\frac{T_2}{T_1} = (3 - 2a^2)^{1/2} \left(\frac{h}{l}\right)^\gamma a^{2\gamma - 2} \tag{7}$$

where h and l are the lengths of the cell and expander regions, respectively. At $a = 1/2$, $h/l = 1/2$, and $\gamma = 5/3$, the relative temperature decrease is found to be $T_2/T_1 \sim 0.2$.

Ion energy extraction requires that ions drift to the ion collector at $\vec{E} \times \vec{B}$. The rate of ion collection is then

$$R_i = n_2 \vec{v}_{E\times B} l \Delta \tag{8}$$

where $\Delta \sim 2d_2$ is the width of the collector electrodes. Since ions bring only perpendicular energy $W_{\perp_2}$ to collection, the rate of energy collection is

$$P_i = n_2 \vec{v}_{E\times B} l \Delta W_{\perp_2} = \frac{a^4}{(3-2a^2)^{1/2}} n_1 k T_1 \frac{E}{B_2} l \Delta \tag{9}$$

Electrons by contrast bring $W_{\parallel_2}$ to the electron collector since they drift parallel to B. Ambipolar considerations require electrons to reach their collector at the same rate that ions reach the ion collector, so that

$$n_2 \vec{v}_{E\times B} l \Delta = n_2 v_{\parallel_{2e}} \Delta^2 \tag{10}$$

so that the electron drift speed is limited to $v_{\parallel_{2e}} = (l/\Delta)\vec{v}_{E\times B}$. The collected electron power is then

$$P_e = n_2 v_{\parallel_{2e}} \Delta^2 \left(\frac{1}{2} m v_{\parallel_{2e}}^2\right) = \frac{a^2 n_1}{(3-2a^2)^{1/2}} \frac{m}{2} \frac{l^3}{\Delta} \left(\frac{E}{B_2}\right)^3 \tag{11}$$

Combining ion and electron power, the total collected power is

$$P = \frac{a^3 n_1}{(3-2a^2)^{1/2}} l d_1 \frac{E}{B_2} \left[2kT_1 + \frac{m}{4}\frac{l^2}{d_1^2}\left(\frac{E}{B_2}\right)^2\right] \tag{12}$$

For $l/d_1 \gg 1$, P peaks at $a \sim \sqrt{3/2}$. Since the maximum for the inverse expansion ratio is 1, expansion is not desirable in this situation. At $a = 1$, there is no adiabatic change in fluid parameters across the expander region, and

$$P = nld\frac{E}{B}(2kT)\left[1 + \frac{m}{8kT}\frac{l^2}{d^2}\left(\frac{E}{B}\right)^2\right] \tag{13}$$

separating the ion and electron contributions, respectively, within the square brackets.

The power input to the converter has two contributions. Thermal flow power from the cell is estimated

$$P_{flow} = 3nkT\sqrt{\frac{kT}{M}}\frac{\pi\Delta^2}{4} \tag{14}$$

and in addition, there is a contribution from the work required of an external agent (power supply) to maintain the electric field in the converter in the presence of particle drifts

$$P_E - n\vec{v}_{E\times B}\Delta l\left(\frac{1}{2}M\vec{v}_{E\times B}{}^2\right) \tag{15}$$

By the mass ratio $M \gg m$, the ion contribution is the only important contribution to this component of input power.

The converter efficiency is defined $\eta = P/P_{in}$ where $P_{in} = P_{flow} + P_E$. Defining a new parameter as the dimensionless drift-to-thermal-speed-ratio, $\alpha = \vec{v}_{E\times B}/v_{th_i}$, the efficiency expression is parameterized as

$$\eta = \frac{1 + \frac{m}{8M}\left(\frac{l}{d}\right)^2\alpha^2}{\frac{3\pi}{2}\frac{d}{\alpha l} + \frac{\alpha^2}{2}} \tag{16}$$

With $l/d \sim 5$ the conversion efficiency peaks at $\eta \sim 70\%$ near $\alpha \sim 1$. This is demonstrated in Fig. 2 as a parameterization of η vs. α with $l/d \sim 5$.

Some additional conditions should be considered. First, to avoid transverse ion loss, it is necessary to ensure $r_{L_i} < \Delta/2$ — the ion gyro-scale fits within the channel dimensions. This requires $B > \sqrt{2kT}/qd \sim 45$ G for 10 eV H^+ ions at $d = 10$ cm, a trivial requirement. More limiting is ensuring a drift time much larger than the ion gyro-time to allow fully developed ion drift flow to intercept the upper electrode $(\Delta VB/E) > \omega_{c_i}^{-1}$. This places an upper limit on $E < \Delta qB^2/M$ of $E, 7600$ V/m when $B = 200$ G. Since $l/d > 1$ is required for $v_{\|_{2e}} > \vec{v}_{E\times B}$, this forces $l \sim 1/2$–1 m. The condition for equal ion and electron contributions to output power is

$$E = \frac{2\sqrt{2}}{5}B\sqrt{\frac{kT}{M}} \sim 15{,}000 \text{ V/m} \tag{17}$$

again for 10 eV and 200 G. This is superceeded by the gyro-time requirement. It is more reasonable then to fix the electric field to a lower value near $\alpha \sim 1$. For example, at $E = 1000$ V/m (e.g. $V =$ 200 V for $\Delta = 20$ cm) and $B = 200$ G at 10 eV, one finds $\alpha \sim 1.6$ and $\eta \sim 54\%$ (from Eq. (16)). The power output under these conditions (and with $n_e \sim 10^{12}$ cm^{-3}), is $P \sim 4.7$ kW.

A reasonable quantity of electric power may be extracted in such a converter design provided, of course, that collisional effects are not important. The effect of collisions has not been considered here. One may estimate, however, as done in the introduction (sec. I) that the magnetization

parameter is quite low for ions, $\Omega_i \ll 1$. This is found even at very high field approaching 1 T. The majority of ions in the stream are then not expected to complete an uninterrupted trajectory to the ion collector. For this reason alone, the success of direct collection in a compact, low power converter would be suspect.

IV. MHD CONVERTER

The MHD converter exploits the Lorentz action on a flowing magnetofluid across a magnetic field to generate an electrical potential difference. A schematic illustrating the basic components of an MHD system interfaced with a CA-plasma cell device is shown in Fig. 3. Magnetofluid flow is extant from the CA-plasma cell (labeled *Plasma Tube-Reactor*) at flow velocity $\vec{u}$. As the flow enters the MDH converter/expansion region, it experiences flow-crossed magnetic field $\vec{B}$. In the absence of an external load, an open-circuit electric field $\vec{E}_o = -\vec{u} \times \vec{B}$ is generated. This is a direct expression of the plasma Ohm's Law when the flow of electric current is prevented. When the system supports the flow of electric current, the relationship between electric current density $\vec{j}$ and $\vec{E}$ (Ohm's law) is given in Eq. (1) where σ is the electrical conductivity of the magnetofluid. The circuit is completed through the external load which reduces the electrode voltage so that $\vec{E} = \kappa\vec{E}_o = -\kappa\vec{u} \times \vec{B}$ where $\kappa < 1$, so that the magnitude of the current density becomes

$$j = \sigma(1 - \kappa)uB \tag{18}$$

The continuous appearance of an MHD voltage, $V = Ed$, (where d is the electrode separation) and electric current flow is predicated upon continuous fluid flow through the channel defined by the separation of the converter electrodes. The flow may be maintained via a pressure drop, ∇P, across the channel so that the plasma component of the fluid is in dynamic equilibrium with the applied field

$$\nabla p = \vec{j} \times B \tag{19}$$

or $\Delta p = jBL$ for a linear pressure drop (*i.e.* constant B, j) across a channel of length L. The converter length required to support the fluid at fixed Δp can then be written

$$L = \frac{\Delta p}{\sigma(1 - \kappa)uB^2} \tag{20}$$

indicating a reduction in scale for concomitant increases in u, B, or σ. When the field magnitude and flow speed are fixed by power and materials limitations, there is a premium on a high degree of conductivity for the fluid. The electrical conductivity in plasma is determined by a number of factors including species, charge, average thermal speed, collision cross section,[33] and B. A detailed analysis on conduction in partially ionized gases will follow (sec. A).

In order to maintain a pressure drop, and hence flow, evacuation of the fluid extant from the converter is required in conventional MHD, but may be unnecessary in the CA-plasma case. Three possible scenarios are presented. (1) The plasma cell and converter may be directly coupled and open to atmosphere in a once-through, *open* system. The pressure drop is maintained by a vacuum pump or by operating at greater than atmospheric pressure. (2) The cell and converter may be arranged in a *closed* configuration which utilizes a recirculating pump to accumulate the converter effluent and divert it back to an injection reservoir in the plasma cell. Neither of the pump scenarios presented in (1) or (2) are beneficial in an energy conversion system since the pumping power required to maintain Δp and hence $\vec{u}$ would necessarily be greater than that converted to electrical power by the flow. This follows directly from the requirement that the energy extracted as electricity is a direct consequence of a high enthalpy fluid expending flow energy in crossing $\vec{B}$. (3) Hot plasma generated in the CA-plasma cell and expanding outward therefrom into the converter region, may introduce an adverse pressure gradient which may be filled by backflow of neutral gas from the converter region returning to the cell. A *natural convection* like pattern may be established providing both continuous flow and refueling simultaneously. The CA-plasma cell and converter may then be coupled in a simply closed configuration without need for pumping.

Power flow through an external load at MHD supported $\vec{j}$ and $\vec{E}$ can be computed

$$P = \vec{j} \cdot \vec{E} = \sigma\kappa(1-\kappa)u^2B^2 \tag{21}$$

This is optimized at $\kappa = 1/2$, which simply represents the impedance matching condition where half the open-circuit voltage drop appears across the load.

A. Electrical Conductivity in an Applied Magnetic Field

As the electrical performance of the MHD converter is a strong function of the electrical conductivity, the accuracy of quantitative determination of σ is of paramount importance. Indeed, when the high concentration of neutral particles is in flow and thermal equilibrium with plasma ions and electrons, it is noted[29] that the MHD efficiency of conversion in historical applications is limited to the ionization fraction. This is a rather debilitating limitation as the ion fraction may be quite low, perhaps at only a few percent or less. However, in the low pressure CA-plasma case, no such equilibrium exists. The greatly reduced collisionality afforded by low density somewhat decouples the plasma species from neutral particles. Input power then is not required to heat the large inventory of neutrals, nor is it required to drive flow in this component so that the input power requirements may be much reduced and the electrical efficiency much greater.

The strong applied magnetic field, on the other hand, does have a dramatic influence on conduction.[34,35] This can be directly ascertained from the electron momentum equation. Under the limiting, yet illustrative, conditions of constant and uniform plasma and flow with $\vec{B} = B\hat{z}$ and $\nabla T_e = 0$, the electron equation of motion yeilds the familiar expression for the transverse electron speed

$$\vec{v}_e = \frac{\Omega_e^2}{1+\Omega_e^2}\frac{E_y}{B} + \frac{\Omega_e^2}{1+\Omega_e^2}\frac{kT_e}{eB}\frac{\nabla_y n_e}{n_e} - \frac{\mu_e}{1+\Omega_e^2}E_x - \frac{D_e}{1+\Omega_e^2}\frac{\nabla_x n_e}{n_e} \tag{22}$$

where $\mu_e = e/(m_e\nu_e)$ is the electron mobility, $D_e = kT_e/(m_e\nu_e)$ is the electron mass diffusivity, and $\Omega_e = \omega_{c_e} = eB/(m_e\nu_e) = \mu_e B$ is the electron magnetization parameter. For $\Omega_e \gg 1$, the electron fluid is magnetized and strongly influenced by $\vec{B}$. When $\Omega_e \ll 1$, the applied field has much less influence than particle collisions on electron transport. The first two terms in Eq. (22) are the familiar electric and diamagnetic drift terms perpendicular to $\vec{B}$. The last two terms represent electrostatic mobility and diffusive transport, yet the magnitude of the transport coefficients is reduced by the factor $1+\Omega_e^2$, so that

$$\mu_{e_\perp} = \frac{\mu_e}{1+\Omega_e^2} \quad , \quad D_{e_\perp} = \frac{D_e}{1+\Omega_e^2} \tag{23}$$

which may represent a significant reduction for large $\vec{B}$. Alternatively, the effective collisionality is increased

$$\nu_{e_\perp} = \nu_e(1 + \Omega_e^2) \ , \quad \eta_{e_\perp} = \eta_e(1 + \Omega_e^2) \tag{24}$$

Because of the mass difference, ions and electrons are influenced by collisions and $\vec{B}$ to differing degrees. Table 2 shows ion and electron collision frequencies with all species present (e, H^+, Ar^o neutrals) for a low power plasma cell possessing conditions of table 1 with 40 eV ions, 10^{12} cm^{-3} plasma density, and a Coulomb logarithm of 20. Charge neutral collisions are among ions or electrons with neutral Ar atoms at 1 Torr total pressure. Coulomb collisions are self (i-i or e-e) or cross (i-e or e-i) involving electrons and H^+ ions as the dominant ionized species. Conduction for both ions and electrons is limited by collisions with neutral particles due principally to the large inventory of neutrals at 1 Torr. These mechanisms (*i.e.* ν_{en}, ν_{in}) will then be considered the only important collisional effects.

In weak magnetic fields ($\Omega_{i,e} \ll 1$), both ions and electrons are relatively unaffected by the presence of $\vec{B}$. Electrons, then, due to their higher mobility, dominate electrical conduction. When the magnetic field strength increases such that $\Omega_{i,e} \gg 1$ (the strong field limit), both ions and electrons are magnetized and electrical conduction perpendicular to $\vec{B}$ is dominated by ion flow. For intermediate fields, as for our test case near $B \sim 1$ T, both ions and electrons conduct electrical current. To see this, a conductivity ratio can be estimated

$$\frac{\sigma_{e_\perp}}{\sigma_{i_\perp}} = \frac{\sigma_e(1 + \Omega_i^2)}{\sigma_i(1 + \Omega_e^2)} \tag{25}$$

At 1 T, $\Omega_e \sim 29.3$ and $\Omega_i \sim 0.27$ (H^+ ions) while $\sigma_e/\sigma_i = \mu_e/\mu_i \sim 85.7$. The conduction ratio perpendicular to $\vec{B}$ then becomes $\sigma_{e_\perp}/\sigma_{i_\perp} \sim 0.1$ so that electrons carry only about 10% of the electrical current in the converter.

B. Sample MHD Converter Performance

MHD converter performance can be illustrated by examining a test case with $B \sim 1$ T, $\kappa = 1/2$, $\Delta p = 1$ Torr, and $u = 1.36 \times 10^4$ m/s (ion acoustic speed at neutral Ar inertia). For $\nu_{e_\perp} = 0.1\nu_{i_\perp}$, and $n_e = 10^{12}$ cm^{-3}, the plasma conductivity perpendicular to $\vec{B}$ is estimated at 0.048 mho/m or

$\eta_\perp \sim 21$ Ω-m. Then employing Eq. (20), a converter length of only ~ 40 cm is found. This is a modest requirement and suggests that such large fields may not be necessary. The MHD electric field generated in this case is $E = \kappa u B \sim 6.8$ kV/m, providing a voltage drop of 680 V across a 10 cm converter gap. The electric current density can then be estimated from Eq. (18) to be ~ 326 A/m^2 so that the MHD output power becomes ~ 8.8 kW.

Sample converter performance is shown in Figs. 4 and 5 illustrating MHD current density and power as functions of applied field, B, from 0–40 T at constant L and u. Though the upper limit on B is clearly impractical, the range encompasses all the relevant MHD physics. Under these constraints the MHD voltage and EMF are linear functions of B. The electric current density (Fig. 4), however, shows much more interesting behavior. There are two peaks in the curve, one at $B \sim 1/\mu_e$ and another at $B \sim 1/\mu_i$, before asymptotically decreasing to zero as $B \to \infty$. This behavior is explained by considering the perpendicular conductivity or mobility of charges in strong B. At low field ($B < 1/\mu_e$), electrons easily conduct under the influence of E, and j increases linearly with B since the MHD E increases with B. As B approaches $1/\mu_e = 0.034$ T, electrons become magnetized and are greatly impeded in their flow perpendicular to B, so that j decreases rapidly. This situation is sometimes referred to as the *ion slip* condition[27] since ions continue to slip through the applied field whereas electrons are trapped. In the region of B parameter space between $1/\mu_e$ and $1/\mu_i$, there is a competition between conductivity reduction and increasing EMF with B. At $B = 1/\mu_i \sim 3.7$ T, ions now become magnetized, and the current once again peaks. Beyond this field strength, the current is a continuously decreasing function of B. The MHD power (Fig. 5) is a continuously increasing function of B in spite of the variation in j with B, since E is continuously increasing. The power function reaches an asymptotic value ($P_\infty = \kappa(1-\kappa)d^2 L u^2 e n/\mu_i \sim 110$ kW for this case) at high field since the E increase is linearly with B and j decreases like B^{-1} at large B.

Though the output power can approach appreciable levels, the quantity of total electric current remains low, $I \leq 25$ A (and $j \leq 600$ A/m^2) so that induced fields remain negligible in comparison with the applied field. The magnetic Reynolds number $R_m = \mu_o \sigma_\perp u d \sim 10^{-5}$ determines the scale

of flow interactions with the applied field. Since $R_m \ll 1$, the complications usually associated with flow-field distortion, hydromagnetic waves, and instabilities can be avoided.

C. Channel Hydrodynamics

The hydrodynamics of one dimensional, steady channel flow ($\vec{u} = u\hat{x}$) in crossed field ($\vec{B} = B\hat{z}$) is examined by considering the conservation equations of hydrodynamics

$$\begin{aligned} \text{energy} &: \rho u \frac{d}{dx}\left(\frac{u^2}{2} + C_p T\right) = \vec{j}\cdot\vec{E} \\ \text{momentum} &: \rho u \frac{du}{dx} + \nabla p = \vec{j}\times\vec{B} \\ \text{continuity} &: \dot{m} = \rho u A = \text{const.} \end{aligned} \tag{26}$$

for a fluid of mass density ρ in a channel of cross section A. If constant flow ($u = \text{const.}$) is considered, the hydrodynamics equations simplify to

$$\begin{aligned} \text{energy} &: \rho u \frac{d}{dx}(C_p T) = \vec{j}\cdot\vec{E} \;\text{ or }\; \frac{dh}{dx} = \frac{\vec{j}\cdot\vec{E}}{\rho u} \\ \text{momentum} &: \nabla p = \vec{j}\times\vec{B} \\ \text{continuity} &: \rho A = \text{const.} \end{aligned} \tag{27}$$

where h is the specific enthalpy.

In considering a constant applied field and disregarding flow distortion of the applied field as indicated by the tiny order of the magnetic Reynolds number, the pressure profile must be linear. By integrating the momentum

$$p(x) = 2j_y BL[1 - x/2L] \tag{28}$$

on $0 \le x \le L$. Given the pressure profile above and ideal gas behavior, $p = nkT$, the energy equation can be integrated to find the temperature profile

$$T(x)/T_o = [1 - x/2L]^{-\frac{kE}{umBC_p}} \tag{29}$$

where T_o is the channel inlet temperature. Since $E = \kappa u B$, the exponent reduces to $\kappa k/mC_p \sim 0.33$ using the properties of Ar as the bulk species. At the channel exit we find $T(L)/T_o \sim 1.26$. The

temperature increase along the channel is attributed to Joule heating of the plasma by the MHD current and field.

Since the temperature and pressure profiles are determined, the density profile can be found

$$\begin{aligned} n(x) &= \frac{2j_y BL}{kT_o}[1 - x/2L]^{1+\frac{kB}{\dot{m}BC_p}} \\ &= n_o[1 - x/2L]^{1.33} \end{aligned} \tag{30}$$

The extant flow (at $x = L$) then has density reduction $n(L)/n_o \sim 0.4$.

By mass conservation, the channel cross section must widen to support constant flow while the density decreases, $A \sim 1/\rho$. Then it is readily determined

$$\begin{aligned} A(x) &= \frac{\dot{m}kT_o}{2j_y BL}[1 - x/2L]^{-(1+\frac{kB}{\dot{m}BC_p})} \\ &= A_o[1 - x/2L]^{-1.33} \end{aligned} \tag{31}$$

As the flow exits the channel, the gap must widen to $A(L)/A_o \sim 2.5$ or $d(L)/d_o \sim 1.6$ to accommodate constant flow.

D. Generator Efficiency and the Hall Effect

The preceding analysis considers only the idealized behavior of an MHD converter, that is the electrodynamic and hydrodynamic behavior in the absence of heat and particle losses, and Hall currents. Collisions, on the other hand, are fully accounted for through the explicit determination of collision frequency and its implementation in the Ohm's Law (Eq. (1)). In this context, the MHD efficiency may be quantified by considering the following. The output power density is determined by the rate at which specific enthalpy in the flow is converted to electrical energy

$$\rho u \frac{dh}{dx} = \vec{j} \cdot \vec{E} = j_y E \tag{32}$$

The rate at which energy is expended is attributed to work done by the fluid in expanding through the applied magnetic field

$$h \frac{dp}{dx} = u j_y B \tag{33}$$

The ratio of these two expressions is the MHD efficiency

$$\eta_{MHD} = \frac{E}{uB} = \kappa \tag{34}$$

This quantity is a constant ($\kappa = 1/2$) in the heretofore provided formalism since no physical effects other than impedance matching are considered.

At high applied field strength, however, the Hall effect may play an important role in channel dynamics.[36–38] The Hall effect in plasma is a consequence of electric current interaction with applied magnetic fields just as that experienced in metalic conductors. In plasma, though, this effect can have significant impact on plasma impedance and dynamics. The Hall effect is quantified via the generalized Ohm's Law

$$\vec{E} + \vec{u} \times \vec{B} = \frac{1}{\sigma}\vec{j} + \frac{1}{en}\left(\vec{j} \times \vec{B} - \nabla p_e\right) \tag{35}$$

where the last two terms were omitted in the form previously employed (Eq. 1). The $\vec{j} \times \vec{B}$ term on the right side is the Hall term. The last term represents the electrodynamic influence of electron pressure gradients and is ignorable when $\beta_e = 2\mu_o k T_e / B^2 \ll 1$. For CA-plasma cell conditions $\beta_e \sim 10^{-6}$ at 1 T so that neglecting electron pressure is well justified.

The Hall contribution, however, is most often not negligible. It can have quite a strong influence on plasmadynamics, electrodynamics, and energy balance in MHD plasmas.[36–38] Via the Hall term, a component of electric current and field perpendicular to B is introduced. For the cartesean MHD channel described earlier with $\vec{B} = (0, 0, B)$ and $\vec{u} = (u, 0, 0)$ resulting in MHD fields E_y and j_y, the Hall contribution appears in the $-\hat{x}$ direction and is given by

$$E_{hall} = E_x = \frac{1}{\sigma} j_x + \frac{1}{en} j_y B \tag{36}$$

where j_x is the Hall current. Lacking experimental guidance or further theoretical constraints on j_x, parameterization is provided by the Morozov[37,38] Hall parameter

$$\Xi = j_x / enu \tag{37}$$

The MHD efficiency expression is then suitably modified to incorporate the rate at which energy is expended in driving Hall currents

$$\eta_{MHD} = \kappa \frac{1}{1 + \frac{j_x E_x}{u j_y B}} \tag{38}$$

No credit is taken here for the potential for power conversion of the Hall current component. This has enhanced performance been suggested elsewhere[27,29] and should be considered further to improve the overall performance of the converter. Figure 6 displays the MHD efficiency including Hall losses as a function of the applied field for $\Xi = 0.1, 0.3, 1.0$. A smaller Hall parameter is clearly desirable here. As Ξ is increased, a greater fraction of converter power is diverted to drive Hall currents. The effect is increased with increasing B since $E_{hall} \sim B$ for large B.

E. Flow

In the absence of spontaneous plasma flow from the hot CA-plasma cell to the relatively cold MHD converter section, a directional plasma flow may also be formed by using a magnetic mirror. A magnetic mirror has a magnetic field gradient in the desired direction of ion flow where the initial parallel velocity of plasma particles increases as the orbital velocity decreases with conservation of kinetic energy and adiabatic invariant $\mu = W_\perp/B$, the linear energy being drawn from that of orbital motion. The adiabatic invariance of flux through the orbit of an ion is a means to form a flow of ions along the field with the conversion of $W_\perp$ to $W_\parallel$.

Plasma is selectively generated in the center region of the CA-plasma power cell. A magnetic mirror located in the center region causes electrons and ions to be forced from a homogeneous distribution of velocities at the cell center to a preferential velocity along the axis of the magnetic mirror. Thus, the plasma ions have a preferential velocity along the field and propagate into the MHD power converter. By preserving the adiabatic invariant, the parallel velocity at any position along the z-axis is given by

$$v_{\parallel_o}^2 = v_o^2 - v_{\perp_o}^2 \frac{B}{B_o} \tag{39}$$

where the zero subscript represents the initial condition at the cell center. In the case that $v_{\parallel_o}^2 = v_{\perp_o}^2 = 0.5 v_o^2$ and $\frac{B}{B_o} = 0.1$ at the MHD power converter, the particle velocity is 95% parallel to the field at the converter.

V. CONCLUSIONS

Preliminary investigation has been made on plasma-to-electric conversion technologies for small to mid-scale CA-plasma cells. Direct electromagnetic and MHD conversion technologies have been considered in some detail for the unique parameter range of CA-plasma cells. The plasma conditions inherent in these devices (intermediate temperature and ionization fraction, high neutral inventory) pose unique challenges to conversion. An $\vec{E} \times \vec{B}$ direct converter is considered in detail showing quite promising ideal performance with conversion efficiency up to $\sim$ 70%. However, in light of the large neutral inventory present, direct conversion including $\vec{E} \times \vec{B}$, other drift concepts, as well as electrostatic collection should be considered as impractical as plasma-to-electric conversion technologies. Collisional interruption of ion trajectories become the most serious shortcoming. However, fluid conversion strategies, like MHD, appear to be much better suited to cell conditions. These conversion technologies do not require charge separation, nor is expansion required in most cases. It is discussed herein that ion acoustic flow at 40 eV can generate up to several kW of electrical power in a 1 T field with conversion efficiency approaching 50% including Hall losses.

References

[1]www.plugpower.com.

[2]Energy Information Administration, *International Electricity Prices for Households*, October 20, 2000 (www.eia.doe.gov/emeu/iea/elecprih.html).

[3]P. Maycock, PV News **19**, 3 (April, 2000).

[4]I. Uehara, T. Sakai, and H. Ishikawa, J. Alloy Comp. **253/254**, 635 (1997).

[5]J. Glanz, New Scientist , 32 (April 15, 1995).

[6]R. L. Mills, N. Greening, and S. Hicks, Optically measured power balances of glow discharges of mixtures of argon, hydrogen, potassium, rubidium, cesium, or strontium vapor, submitted to Int. J. Hydrogen Energy, 2001.

[7]R. L. Mills, P. Ray, B. Dhandapani, and J. He, Spectroscopic identification of fractional rydberg states of atomic hydrogen, submitted to J. Phys. Chem. Letts., 2001.

[8]R. Mills, J. Dong, W. Good, P. Ray, J. He, and B. Dhandapani, Measurement of energy balances of noble gas-hydrogen discharge plasmas using calvet calorimetry, submitted to Int. J. Hydrogen Energy, 2001.

[9]R. L. Mills, P. Ray, B. Dhandapani, M. Nansteel, X. Chen, and J. He, New power source from fractional quantum energy levels of atomic hydrogen that surpasses internal combustion, Spectrochimica Acta, in progress, 2001.

[10]R. L. Mills, P. Ray, B. Dhandapani, and J. He, Comparison of excessive balmer line broadening of glow discharge and microwave hydrogen plasmas with certain catalysts, submitted to J. Phys. Chem., 2001.

[11]R. L. Mills, A. Voigt, P. Ray, M. Nansteel, and B. Dhandapani, Measurement of hydrogen balmer line broadening and thermal power balances of noble gas-hydrogen discharge plasmas, Int. J. Hydrogen Energy, in press, 2001.

[12]R. L. Mills, Blacklight power technology-a new clean energy source with the potential for direct conversion to electricity, in *Global Foundation International Conference on Global Warming and Energy Policy*, Fort Lauderdale, FL, 2000, Kluwer Academic/Plenum Publishers, New York.

[13]R. L. Mills, Blacklight power technology-a new clean hydrogen energy source with the potential for direct conversion to electricity, in *Proceedings of the National Hydrogen Association, 12th Annual U.S. Hydrogen Meeting and Exposition, Hydrogen: The Common Thread*, Washington, DC, 2001.

[14]R. G. Mills, Nucl. Fusion **7**, 223 (1967).

[15]D. L. Rose, Nucl. Fusion **9**, 183 (1969).

[16]G. H. Miley, *Fusion Energy Conversion*, American Nuclear Society, La Grange, IL, 1976.

[17]R. W. Moir, W. L. Barr, and G. A. Carlson, Direct conversion of plasma energy to electricity for mirror fusion reactors, in *Proc. 5th IAEA Conference on Plasma Physics and Controlled Nuclear Fusion Research*, Japan, 1974, 1975, IAEA, IAEA Pub., Vienna.

[18]R. W. Moir and W. L. Barr, Nucl. Fusion **13**, 35 (1973).

[19]R. P. Freis, Nucl. Fusion **13**, 247 (1973).

[20]J. D. Lee, J. Nucl. Mater. **53**, 76 (1974).

[21]R. W. Moir, W. L. Barr, and G. H. Miley, J. Nucl. Mater. **53**, 86 (1974).

[22]A. V. Timofeev, Sov. J. Plasma Phys. **4**, 464 (1978).

[23]V. M. Glagolev and A. V. Timofeev, Plasma Phys. Rep. **19**, 745 (1994).

[24]S. Way, Westinghouse Eng. **20**, 105 (1960).

[25]M. Sakuntala, B. E. Clotfelter, W. B. Edwards, and R. G. Fowler, J. Appl. Phys. **30**, 1669 (1959).

[26]H. P. Pain and P. R. Smy, J. Fluid Mech. **10**, 51 (1961).

[27]R. J. Rosa, Phys. Fluids **4**, 182 (1961).

[28]R. J. Rosa, J. Appl. Phys. **31**, 735 (1961).

[29]C. Mannal and N. W. Mather, *Engineering Aspects of Magnetohydrodynamics*, Columbia University Press, NY, 1962.

[30]R. B. Clark, D. T. Swift-Hook, and J. K. Wright, Brit. J. Appl. Phys. **14**, 10 (1963).

[31]P. R. Smy, J. Appl. Phys. **32**, 1946 (1961).

[32]F. Bitter, Rev. Sci. Instrum. **7**, 479 (1936).

[33]S. C. Brown, *Basic Data of Plasma Physics*, The Technology Press of The Massachusetts Institute of Technology and John Wiley and Sons, Inc., New York, 1959.

[34]H. J. Pain and P. R. Smy, J. Fluid Mech. **9**, 390 (1960).

[35]M. Sakuntala, A. von Engel, and R. G. Fowler, Phys. Rev. **118**, 1459 (1960).

[36]D. C. Black, R. M. Mayo, and R. W. Caress, Phys. Plasmas **4**, 2820 (1997).

[37]D. C. Black, R. M. Mayo, R. A. Gerwin, K. F. Schoenberg, J. T. Scheuer, R. P. Hoyt, and I. Henins, Phys. Plas. **1**, 3115 (1994).

[38]K. F. Schoenberg, R. A. Gerwin, I. Henins, R. M. Mayo, J. T. Scheuer, and G. Wurden, IEEE Trans. Plas. Sci. **21**, 625 (1993).

[a)]Electronic mail: rmayo@blacklightpower.com

Table 1: Typical plasma conditions in Ar-H CA-plasma cell with 5% minority H concentration.

Electron Temperature	T_e	10 eV
Ion Temperature	T_i	30–40 eV
Plasma Density	$n_e = n_i$	10^{12}–10^{14} cm^{-3}
Majority Neutral Density	n_{Ar}	3×10^{16} cm^{-3}
Minority Neutral Density	n_H	1.5×10^{15} cm^{-3}

Table 2: Ion and electron collision frequencies in a CA-plasma cell having the conditions of table 1 with 40 eV H^+ ions, 10^{12} cm^{-3} plasma density, and Coulomb logarithm of 20.

	Neutrals	Electrons	Ions
	ν_{xn} s^{-1}	ν_{xe} s^{-1}	ν_{xi} s^{-1}
Electrons	6×10^9	2.7×10^6	2.7×10^6
Ions	3.8×10^8	2×10^3	7.8×10^3

Figures

FIG. 1. $\vec{E} \times \vec{B}$ type direct converter schematic.

FIG. 2. Ideal efficiency for an $\vec{E} \times \vec{B}$ converter as a function of drift to thermal ratio α with $l/d \sim 5$.

FIG. 3. Schematic of an MHD converter interfaced to a CA-plasma cell, labeled *Plasma Tube-Reactor*. A magnetic mirror coil provides a guide field for the plasma flow extant from the cell region.

FIG. 4. MHD converter current density for sample converter as a function of applied magnetic field strength.

FIG. 5. MHD converter power density for sample converter as a function of applied magnetic field strength.

FIG. 6. MHD converter efficiency as a function of applied magnetic field strength including Hall losses for $\Xi = 0.1, 0.3, 1.0$.

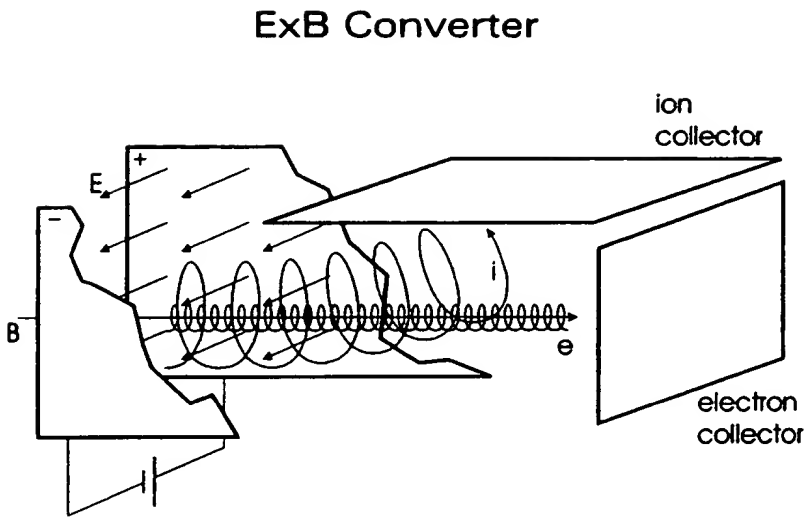

Figure 1

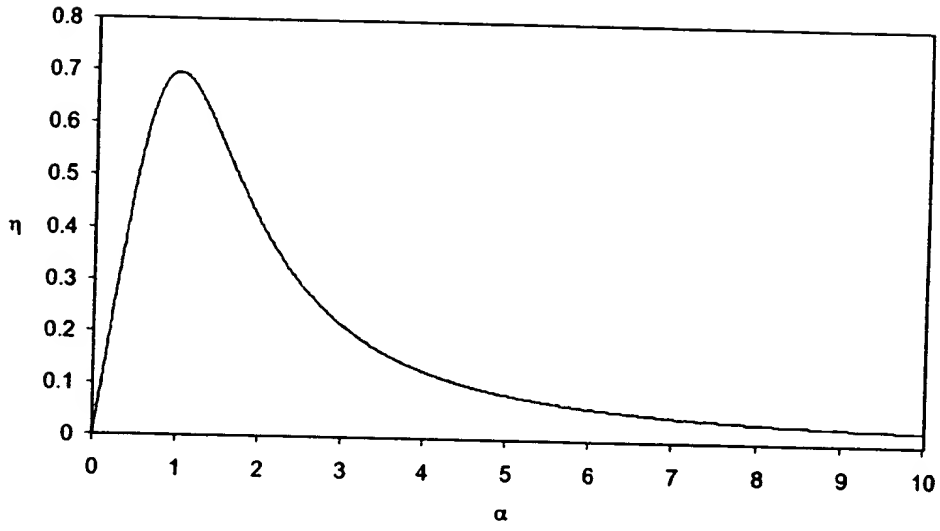

Figure 2

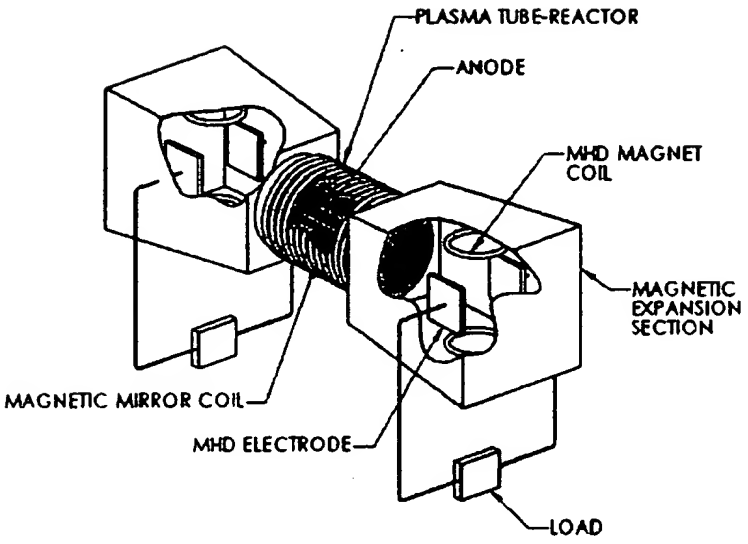
PLASMA TUBE-REACTOR
ANODE
MHD MAGNET COIL
MAGNETIC EXPANSION SECTION
MAGNETIC MIRROR COIL
MHD ELECTRODE
LOAD

Figure 3

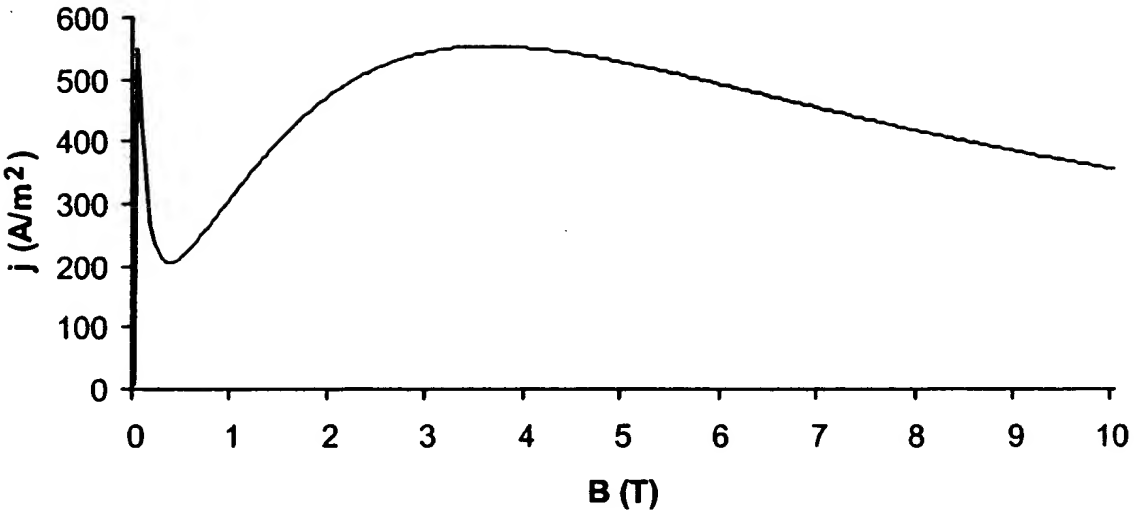

Figure 4

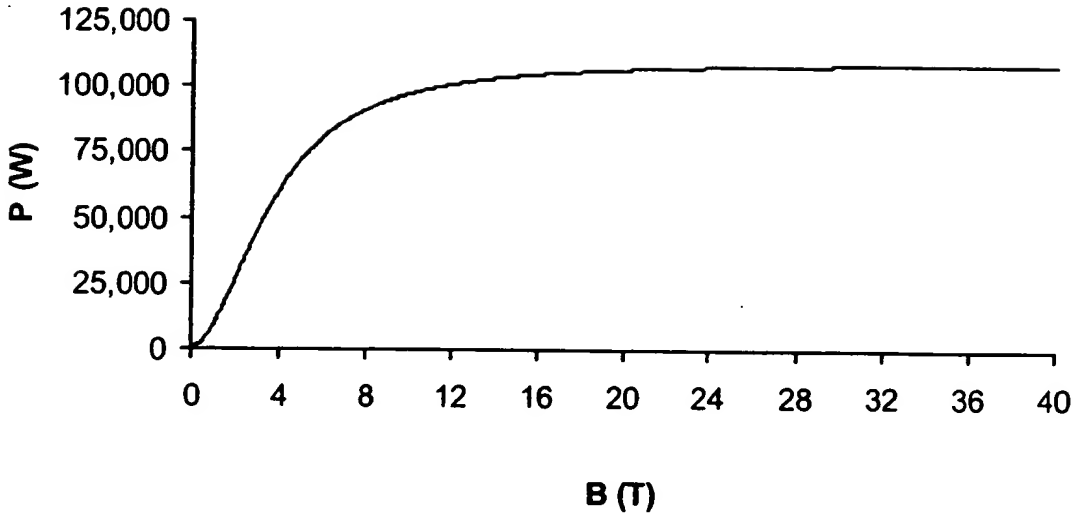
125,000
100,000
75,000
50,000
25,000
0
P (W)
0
4
8
12
16
20
24
28
32
36
40
B (T)

Figure 5

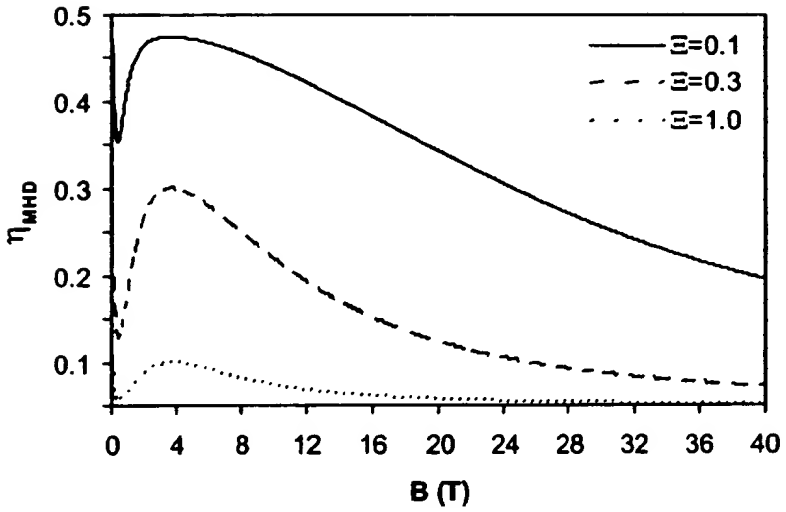

Figure 6